

Exploiting P-S converted waves: Part 1, Modeling the effects of anisotropy and heterogeneities

Reinaldo J. Michelena*, Elias Ata, and Jesús Sierra, *Intevep S.A.*

DP1.2

SUMMARY

We performed extensive modeling studies to evaluate P-S converted waves effectiveness and limitations in the estimation of both cracks orientation and density. The target area is a fractured, carbonate reservoir located in south-west Venezuela. The reservoir depth is on the order of 3000 m, which implies that high quality P-S data are needed to obtain detectable information about the anisotropy at this depth. We focused our analysis on P-S converted waves because only explosives charges were available as energy sources. The modeling was performed prior to and after the data acquisition to help both design of the experiment and interpretation of the data. Synthetic seismograms were generated using 2D, elastic finite difference, along with a 3D-3C, paraxial ray tracing codes. We conducted also a noise-spread test to complement this study and determine the acquisition parameters.

A 3D velocity model of the subsurface was built based on previous P-wave seismic sections, well logs (dual-sonic, density, check-shots and FMS), geological maps, and production information. This model was perturbed in a layer stripping fashion until an acceptable match was obtained around the depth of interest between synthetic and multicomponent field data. Then, anisotropy was introduced to quantify the effect on the converted waves of both vertical fractures and fine horizontal layering within the reservoir volume. The anisotropy produced measurable differences in traveltimes and amplitudes between in-line and cross-line components. These differences (which are comparable to those observed on the field data) suggest that it is feasible to map fractures at depths around the reservoir area by using P-S converted waves.

INTRODUCTION

Modeling studies prior to implementing a seismic field survey can help define acquisition parameters, weigh limitations, and shed some light on what to be expected from the data in the analysis stage. An effective modeling approach is one that consists of both adequate modeling tools and 3D models that are close representation of the subsurface volume to be studied. A modeling algorithm that computes the full elastic wavefield (Etgen, 1987) together with a paraxial ray tracing algorithm (Gibson et al., 1991; Beydoun and Keho, 1987) can help identify the events and emphasize the effects of perturbing the model parameters. In addition, effects of anisotropy and heterogeneities may be isolated and realistic constraints may be imposed on the physical parameters.

This study was performed to investigate the effectiveness of P-S converted waves in mapping cracks density and orientation (Crampin, 1981; Thomsen, 1988) in a fractured carbonate reservoir 3000 m deep. The site is located in south-west Venezuela. The initial isotropic, 3D model was based on exact

physical locations and parameters obtained from maps, P-wave seismic sections, well logs, geological models, and production information. As no previous S-wave information was available (except at one well), a noise-spread test was conducted to complement and provide more control on the modeling results and to help design the acquisition. Anisotropy was introduced in various formations around the reservoir, at different stages, and 2D profiles of various azimuths were evaluated and compared with the field data. We concluded that the data are sensitive to anisotropy within formations around the reservoir. Results of this study helped the design, recording, and interpretation of a high resolution P-S converted wave data set (Ata et al., 1994).

MODELING TOOLS

The modeling tools used to perform this exercise were paraxial ray tracing in 3D inhomogeneous anisotropic media (Gibson et al., 1991) and finite difference in 2D, transversely isotropic media (Etgen, 1987). The 3D paraxial ray tracing was used to identify events and evaluate 3D effects on the 2D seismograms. The 2D finite difference provided the full elastic wavefield seismograms that we used to compare with the field data. The surface and all other boundaries of the model were set to be absorbing to facilitate the identification of the reflection events in the data generated with finite difference.

VELOCITY MODEL

The 3D input model for the ray tracing code is described by layers of irregular interfaces that contain interpreted geological features such as faults, folds and dips. If a particular layer is anisotropic, the 21 elastic constants that control the wave propagation at all angles need to be specified. In this paper, however, we considered only isotropic and transversely isotropic models with vertical and horizontal axes of symmetry. A 2D, pixel-based slice of the 3D model along a chosen azimuth is the input to the finite difference code.

We built the model using interpreted P-wave time sections, check shots from two wells, P- and S-wave velocity logs recorded around the reservoir, density logs, and time contour maps of two interfaces in the reservoir. Fig. 1 shows the location of the P-wave lines and the wells where log information was available. In this figure, black, thick lines show the location of the P-wave sections. The multicomponent data were recorded along the dashed, thick lines. Black, thick dots represent the wells where velocity information was available. Well logs from these and other wells (grey, thin dots) will be used for interpretation and calibration purposes.

One example of the P-wave sections used is shown in Fig. 2. The most relevant events are the top of a shale and sand intervals (mid eocene) and the top of the carbonate reservoir (cre-

taceous). These three events are marked as A, B, and C respectively. Time maps of events B and C, and all events interpreted in the P-wave sections were converted to depth by using velocities derived from check shots. Fig. 3 shows the position of all the major interfaces in the model after depth conversion. No lateral velocity variations were introduced within individual layers and in places where no information was available, the given data were extended smoothly horizontally as well as in depth.

DATA ACQUISITION

Three 10 000 m, multicomponent lines were centered over the reservoir along three different azimuths (Fig. 1). The three lines intersect different well locations that will be used for control and calibration of the results. The survey was designed to maximize the data quality with respect to resolution and signal-to-noise ratio (S/N). A noise test was performed along a portion of line 3C-3 in order to select the proper recording parameters. We analyzed carefully the noise test data to determine, first, the spatial sampling interval required to prevent aliasing of surface waves and, second, the offsets required to observe P-S conversions without noise contamination. We made also various tests to determine the optimum depth of the explosive charge that minimizes the effect of the near surface. More details about the data acquisition can be found in Ata et al. (1994).

The noise test and the modeling were done in parallel. Although the modeling predicted that it was possible to measure converted waves within the offsets proposed, the results of the modeling and the field data didn't agree well and, therefore, to produce better agreement the original velocity model was modified accordingly. Although the modeling could help us in certain aspects of the field survey (resolution, offsets), missing information when building the model and algorithm limitations prevented accurate predictions of the actual survey parameters. These parameters were determined from the noise-spread test data.

Fig. 4 shows field seismograms of the in-line, cross-line, and vertical components for a shot point located at the intersection of the three multicomponent lines (Fig. 1) with receivers deployed along line 3C-3. High S/N P-P reflections can be clearly seen on the vertical component while P-S reflections can be observed on both horizontal components. The presence of shear energy on both components is explained in the following section.

MODELING RESULTS

In addition to acquisition design, we did modeling to interpret the different events seen in the field records along the different azimuths, for a shot located at the intersection of the three lines. The source wavelet was a second derivative of a gaussian curve, with frequencies between 5 and 30 Hz. To avoid numerical dispersion and to ensure stability in the finite difference modeling, the sampling interval and the grid size were chosen to be 0.001 set and 10×10^2 respectively.

The velocities within layers in the model of Fig. 2 were modi-

fied in a layer stripping fashion in order to match the events observed in the field data. Fig. 5 shows the result of the 2D finite difference modeling. Synthetic and field data agree well in the zone of interest, for both in-line and vertical components. The P-S conversions observed at and below 3 sec occur at the depths in the model where the shear velocity contrasts are the largest. These conversions and other strong events seen in the horizontal and vertical components come from the zone of interest around the reservoir.

In a layered isotropic medium, explosive sources don't produce energy in the cross-line component. Deviations from such a medium caused either by heterogeneities or anisotropy with axis of symmetry oriented out of the plane of the survey, can produce energy in the cross-line component. If the plane of incidence is not perpendicular to the conversion surface, energy may be observed in the cross-line component. Energy in the cross-line component may be observed also when the axis of symmetry and the azimuth of the multicomponent line are neither parallel nor perpendicular to each other, which can be the case when the orientation of the fractures and their axes of symmetry are different from the orientation of the line. In this situation, the shear energy splits right after being converted from compressional energy.

Traveltime differences can be used to determine whether the P-S conversions observed in the cross-line directions are caused by anisotropy or heterogeneity. If the cross-line energy is generated by heterogeneities, converted waves in the cross-line direction arrive at the same time as those recorded on the in-line component. However, if the cross-line energy is produced by azimuthal anisotropy, the energy in both components arrive at different times (Thomsen, 1988).

Fig. 6, generated with ray tracing, can be used to explain the origin of the energy observed in the cross-line direction in the field data. When the model is isotropic most of the converted wave energy is recorded along the in-line component (Fig. 6a). A little energy produced by heterogeneities is recorded in the cross-line and vertical components (Figs. 6b and 6c). When azimuthal anisotropy is introduced in the layer right below event A, we see energy of similar amplitude in both horizontal components (Figs. 6d and 6e) with traveltime differences on the order of 10 to 15 ms. We conclude from this result that the heterogeneities in this particular model are not able to produce conversions with comparable energy in both cross-line and in-line components. Consequently, the converted wave energy observed in the cross-line component is generated by azimuthal anisotropy, even in cases when traveltime differences are too small to be detected. This result shows that is possible to use the converted P-S waves to map azimuthal anisotropy in the zone of interest around 3000 m.

CONCLUSIONS

At the site where we conducted the multicomponent experiment, P-SV converted waves generated at depth of 3000 m contain measurable information about anisotropy. The most clear evidence of azimuthal anisotropy around the depths of interest is that converted waves energy is seen in both horizontal components instead of the in-line component only,

which is what we expect when the source is explosive and the medium is horizontally stratified. We have shown that the deviations from layered media of the structures at this site are not responsible for the generation of converted energy with amplitudes similar to those received along the in-line direction.

A more careful analysis of the traveltime and amplitude differences between arrivals recorded in the two horizontal components reveals also that after the conversion, the shear waves traveled across azimuthally anisotropic rocks. These differences are analyzed in a companion paper (Ata et al., 1994) to characterize the azimuthal anisotropy around the reservoir.

We plan to introduce lateral velocity variations in the model by incorporating the results of the velocity analysis of the multicomponent records. Then, this model will be interpreted in terms of a fracture model (Hudson, 1981; Thomsen, 1993) to obtain additional information about the characteristics of the fractures.

ACKNOWLEDGMENTS

Thanks to Corpoven, S. A. and Intevp, S.A. for their support and permission to publish this work. The help of Maria Donati in building the model is also gratefully acknowledged.

REFERENCES

- Ata, E., Michelena, R. J., Gonzalez, M., Cerquone, H., and Carry, M., 1994, Exploiting P-SV converted waves in mapping fractures: Part 2. Application to a fractured reservoir: 64th Ann. Internat. Mtg., Soc. Expl. Geophys., Expanded Abstracts.
- Crampin, S., 1981, Review of wave motion in anisotropic and cracked elastic media: *Wave Motion*, 3, 343-391.
- Beydoun, W., and Kebo, T., 1987, The paraxial ray method: *Geophysics*, 52, 1639-1653
- Etgen, J. T., 1987, Finite difference elastic anisotropic wave propagation: *Stanford Expl. Proj. SEP-56.23-57*.
- Gibson, R. L., Sena, A. G., and Toksoz, M. N., 1991, Paraxial ray tracing in 3D inhomogeneous, anisotropic media: *Geoph. Prosp.*, 39, 473-504.
- Hudson, J. A., 1981, Wave speeds and attenuation of elastic waves in material containing cracks: *Geophys. J. R. Astr. Soc.*, 66, 133-150.
- Thomsen, L., 1988, Reflection seismology over azimuthally anisotropic media: *Geophysics*, 53, 304-313.
- Thomsen, L., 1993, Elastic anisotropy due to aligned cracks in porous rocks: submitted for publication *Geophys. Prosp.*

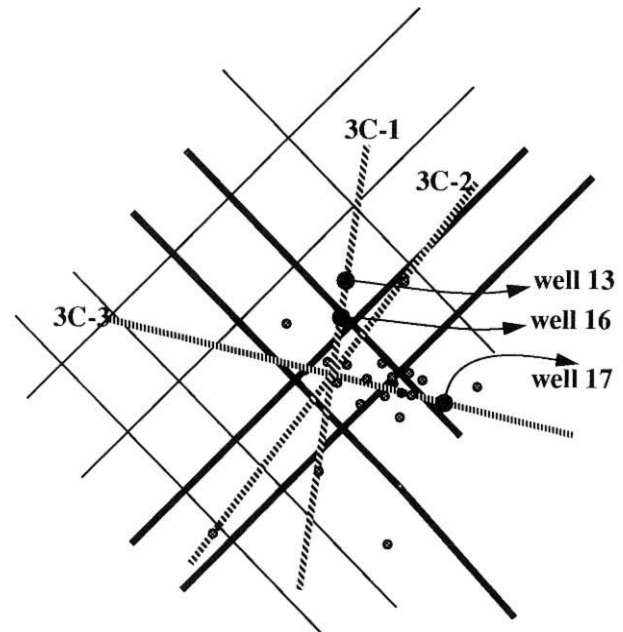


Figure 1. Location of the P-wave sections (black, thick lines) and wells (black, thick dots) used to built the 3D, velocity model. The multicomponent data were recorded along the lines 3C-1, 3C-2, and 3C-3. Each multicomponent line is 10 000 m long.

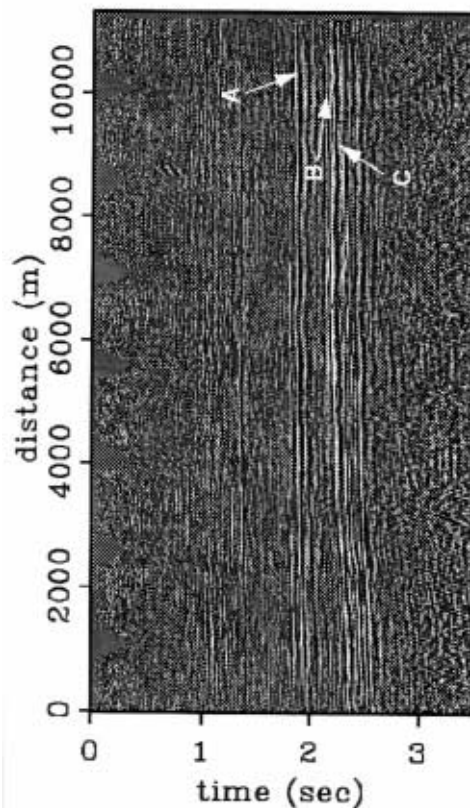


Figure 2. Example of one of the P-wave, time sections used to built the model. The events of interest are marked with A, B, and C. C is the top of the (carbonate) reservoir.

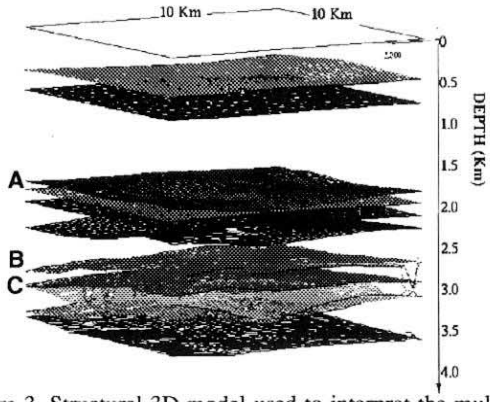


Figure 3. Structural 3D model used to interpret the multicomponent data. Only horizons B and C come from depth-conversion of time maps.

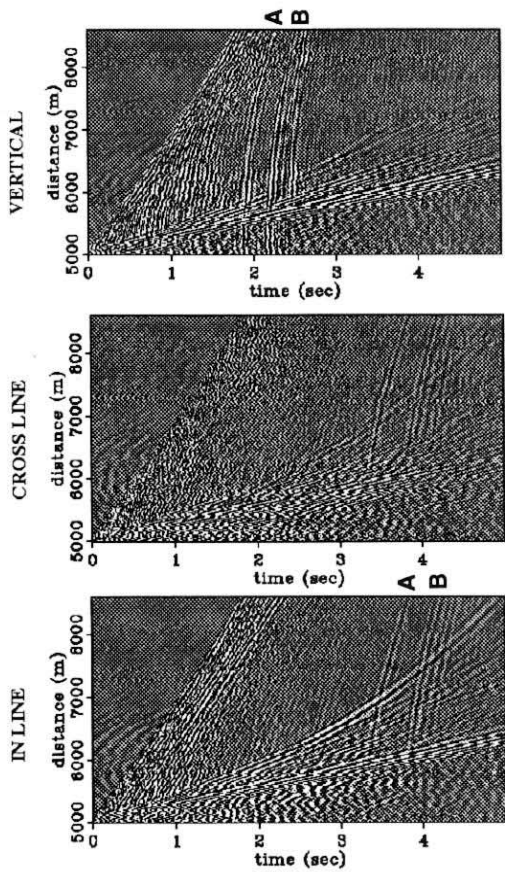


Figure 4. Field, shot gathers for a source located at the intersection of the three multicomponent lines and the receivers on line 3C-3 (Fig. 1). P-S reflections are clear in both in-line and cross-line horizontal components. Reflections from horizons A and B are shown for reference.

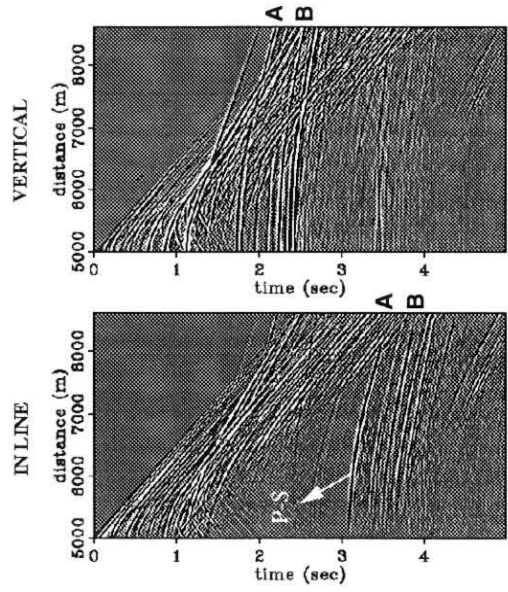


Figure 5. Synthetic, shot gather generated with finite difference for source located at the intersection of the three lines and the receivers in the direction of line 3C-3 (Fig. 1). P-P and P-S reflections around the depths of interest are similar to the ones observed in the field data (Fig. 4).

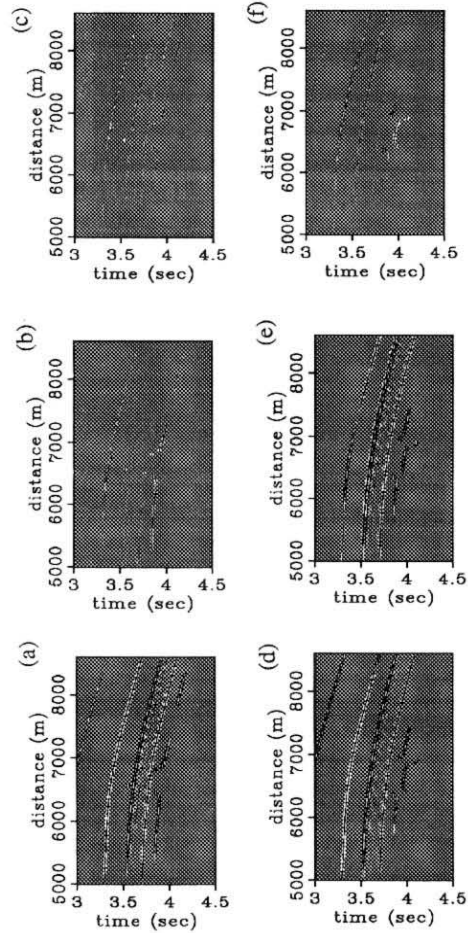


Figure 6. Synthetic, shot gather generated with ray tracing. Only the events around the P-S conversions are shown. (a) Isotropic model, in-line component. (b) Isotropic model, cross-line component. (c) Isotropic model, vertical component. (d) Azimuthally anisotropic model, in-line component. (e) Azimuthally anisotropic model, cross-line component. (f) Azimuthally anisotropic model, vertical component.